ELSEVIER

Journal of Neuroscience Methods 137 (2004) 321–332

JOURNAL OF NEUROSCIENCE METHODS

www.elsevier.com/locate/jneumeth

Fourier-, Hilbert- and wavelet-based signal analysis: are they really different approaches?

Andreas Bruns*

Neurophysics Group, Physics Department, Philipps University, Renthof 7, D-35032 Marburg, Germany

Received 3 December 2003; received in revised form 20 February 2004; accepted 2 March 2004

Abstract

Spectral signal analysis constitutes one of the most important and most commonly used analytical tools for the evaluation of neurophysiological signals. It is not only the spectral parameters per se (amplitude and phase) which are of interest, but there is also a variety of measures derived from them, including important coupling measures like coherence or phase synchrony. After reviewing some of these measures in order to underline the widespread relevance of spectral analysis, this report compares the three classical spectral analysis approaches: Fourier, Hilbert and wavelet transform. Recently, there seems to be increasing acceptance of the notion that Hilbert- or wavelet-based analyses be in some way superior to Fourier-based analyses. The present article counters such views by demonstrating that the three techniques are in fact formally (i.e. mathematically) equivalent when using the class of wavelets that is typically applied in spectral analyses. Moreover, spectral amplitude serves as an example to show that Fourier, Hilbert and wavelet analysis also yield equivalent results in practical applications to neuronal signals.

Keywords: Spectral analysis; Time–frequency analysis; Amplitude; Phase; Analytic signal; Coherence; Phase synchrony; Envelope correlation

1. Introduction

Many studies in neurosciences include the measurement and evaluation of dynamic electromagnetic physiological parameters (measured, e.g., with electro-/magnetoencephalography, electrocorticography, electroretinography, electrooculography, electromyography or electrocardiography or microelectrodes). While the analysis of such neurophysiological signals increasingly often incorporates model-based (e.g., autoregressive) or information-theoretic approaches, extensive use is also still made of traditional spectral analysis techniques in which amplitude and phase values are directly estimated from a time–frequency transform of the measured signal. It has long been known, for example, that the spectral composition of electrical brain signals depends on the current state of the brain (Adrian and Matthews, 1934; Berger, 1929). Motivated by this fact, classical electroencephalography has been using an empirical subdivision of the frequency axis into separate *bands* or ranges (δ, ϑ, α, β, γ). If one wants to characterize not only different general states, but also the dynamics of neuronal processes, this requires a time-resolved (e.g., *event-related*) spectral analysis. Currently, three different classical approaches to time–frequency analysis—Fourier, Hilbert and wavelet approach—are very prevalent in the neuroscience community. Any of these methods yields quantities which can serve as a basis for further analyses. In particular, some of the most common coupling or synchrony measures (like coherence or phase synchrony) can be derived from the results of these spectral analysis techniques.

Certainly, the *Fourier transform* can be said to constitute the most widely used operation to obtain a spectral representation of a given signal. And if the Fourier approach is used in combination with a sliding time window (*short-time Fourier transform*), a spectro-temporal representation of the signal is obtained, which allows tracking of the temporal evolution of spectral values. During the last one or two decades, however, two other approaches have increasingly often been applied in neurophysiological signal analysis. Firstly, the idea of the *wavelet transform* is to convolve the signal to be analyzed with several oscillatory filter kernels representing different frequency bands, respectively. Secondly, the *Hilbert transform* can be used to determine the instantaneous, so-called *analytic* amplitude and phase of a given bandpass signal.

* Tel.: +49-711-17-41936; fax: +49-711-3052-167738.
E-mail address: andreas.a.bruns@daimlerchrysler.com (A. Bruns).

0165-0270/$ – see front matter © 2004 Elsevier B.V. All rights reserved.
doi:10.1016/j.jneumeth.2004.03.002

In several fields, the notion appears to have become more and more established that spectral analyses based on Hilbert or wavelet transforms yield better time–frequency resolutions or are less susceptible to non-stationarity than Fourier-based analyses. But this is actually not the case. The present paper is meant as a tutorial report in order to demonstrate that Fourier, Hilbert and wavelet transforms and their derived parameters are formally equivalent and that results are essentially the same as long as the relevant analysis parameters are matched with each other.

2. Spectral parameters and derived measures

In the following, let $s(t)$ be the neurophysiological signal of interest. A time-resolved spectral analysis of this signal will yield a time-dependent spectrum $S(f,t)$, i.e., a two-dimensional representation of the signal in time–frequency product space. Such a spectro-temporal representation is complex-valued, i.e., at each point, it consists of an *amplitude* value $|S(f,t)|$ and a *phase* value $\varphi(f,t)$, such that

$$S(f,t) = |S(f,t)| \cdot e^{i\varphi(f,t)}. \quad (1)$$

In other words, in order to estimate at a certain time t and frequency f the signal's amplitude and/or phase, as well as more sophisticated amplitude- and/or phase-based parameters (e.g., coupling measures like coherence), one first needs to determine the above complex-valued spectro-temporal representation. Three different approaches to this end will be reviewed in detail in Section 3.

After having determined the signal's spectro-temporal representation $S(f,t)$, a variety of parameters can be estimated from it. In many situations, the signal is repeatedly measured under identical external conditions, yielding N different *realizations* or *single trials* $s_n(t)$, $n = 1, \ldots, N$, from which the ensemble expectation values of the desired parameters can be estimated. In the following, the single-trial number will be indicated by a subscript n for all quantities.

2.1. Amplitude

One of the most frequently determined signal parameters certainly is spectral *amplitude*. When squared, it becomes spectral *power*, and it constitutes the basis of such widely used measures as, e.g., event-related synchronization or depression (ERS or ERD), (induced) band power, time–frequency energy, and many others.

As can be seen from Eq. (1), the signal's amplitude is easily obtained as the modulus (the absolute value) of the spectro-temporal representation. If amplitude is to be estimated independently of trial-to-trial phase variations, this step is performed individually for each single trial:

$$A_n(f,t) = |S_n(f,t)|. \quad (2)$$

Subsequent estimation of the ensemble mean, i.e. the expectation value of the signal's amplitude spectrum, is then achieved by simple averaging:

$$A(f,t) = \frac{1}{N}\sum_{n=1}^{N} A_n(f,t). \quad (3)$$

Another possibility to determine a spectral estimator is to smooth a single-trial spectrum by averaging over neighboring values within a certain frequency interval, which is formally equivalent to (frequency-domain) convolution of the raw spectrum with a kernel that has to be specified in detail. As such smoothing reduces resolution in the frequency domain, the raw spectrum initially has to possess the M-fold resolution of the actually desired resolution Δf, where M is the effective number of raw values contributing to one smoothed value, respectively. As a consequence of time–frequency uncertainty, this fact in turn requires an M-fold coarser temporal resolution. Under these circumstances, capturing the dynamics of fast processes becomes difficult, for which reason this type of estimation is not appropriate to many situations.

2.2. Phase

Analogously to the previous section, also the signal's phase can be extracted from the complex-valued spectro-temporal representation. According to Eq. (1), phase is simply the complex argument of $S(f,t)$:

$$\varphi_n(f,t) = \arg(S_n(f,t)). \quad (4)$$

Unlike with amplitude, however, it is relatively unusual in neuroscience to estimate ensemble expectation values of phase spectra per se. Instead, it is much more common to use phase information for quantifying coupling between signals recorded simultaneously on different *channels* (e.g., at different sites of the brain). In particular, phase *differences* between two channels are often incorporated into phase-sensitive coupling measures, which will be treated in the following section.

2.3. Coupling measures

In order to investigate the connectivity among different (central and/or peripheral) neuronal populations, it is often helpful to quantify statistical interdependencies among the neurophysiological signals measured at different sites. In this report, the focus will be on three coupling measures that can be derived from the signals' spectro-temporal representations according to Eq. (1). In detail, these will be (i) *coherence*, which incorporates both amplitude and phase information (Section 2.3.1), (ii) *phase consistency*, which only regards the signals' phasing (Section 2.3.2), and (iii) *amplitude envelope correlation*, which is solely amplitude-sensitive and has been scarcely noticed up to now (Section 2.3.3).

In the following, let us assume that signals have been measured at two different sites X and Y of the neurophysiological system under consideration. As with the single-trial number n, the two sites or channels will be indicated by subscripts, e.g., $s_{X,n}(t)$ and $s_{Y,n}(t)$ ($n = 1, \ldots, N$).

2.3.1. Coherence

Coherence is a normalized spectral measure which quantifies linear coupling between two signals $s_X(t)$ and $s_Y(t)$. It becomes zero when the signals are linearly independent, and unity when they are perfectly coherent. Signals are "perfectly coherent" at a given frequency when they have both constant phase difference and constant amplitude ratio over the time considered. Note that neither the phase difference need be zero nor the amplitude ratio need be unity.

Generally, (squared) coherence is defined as (Bendat and Piersol, 1971)

$$\kappa^2_{XY}(f) = \frac{|\langle S_X(f) \cdot S^*_Y(f)\rangle|^2}{\langle |S_X(f)|^2\rangle \cdot \langle |S_Y(f)|^2\rangle}, \tag{5}$$

where $S_X(f)$ and $S_Y(f)$ denote the signals' complex-valued spectra, the superscript '*' denotes complex conjugation, and $\langle\cdot\rangle$ denotes the statistical expectation value.

Like in Section 2.1, expectation values can be estimated by averaging over realizations of an ensemble or, alternatively, by smoothing in the frequency domain. In the former case, which is the preferred procedure here (cf. Section 2.1), Eq. (5) becomes:

$$\kappa^2_{XY}(f,t) = \frac{\left|\sum_{n=1}^{N} S_{X,n}(f,t) \cdot S^*_{Y,n}(f,t)\right|^2}{\sum_{n=1}^{N}|S_{X,n}(f,t)|^2 \cdot \sum_{n=1}^{N}|S_{Y,n}(f,t)|^2}. \tag{6}$$

The estimator according to Eq. (6) is consistent, but it has a systematic bias in so far as for finite sample sizes N, its expectation value is non-zero even for completely independent signals. According to Benignus (1969), the bias correction is given by

$$\kappa^2_{XY}(f,t) \to \kappa^2_{XY}(f,t) - \frac{1-\kappa^2_{XY}(f,t)}{N}. \tag{7}$$

For better comparability with correlation values (e.g., Section 2.3.3), it is sometimes advisable to use *unsquared* coherence $\kappa_{XY}(f,t)$ instead of squared coherence $\kappa^2_{XY}(f,t)$.

Amplitude and phase contributions are not equally important in computing coherence. Phase coupling is both necessary and sufficient to yield non-zero coherence. Amplitude coupling, by contrast, is merely able to further increase coherence values which are already non-zero due to phase coupling. Amplitude coupling per se is not sufficient to yield high coherence, because independent phases will always make coherence vanish, regardless of any amplitude correlation. On the other hand, even independent amplitudes will always yield non-zero coherence (provided that the phases are coupled), because correlation of the (by definition) positive amplitudes is always greater than zero (cf. also Section 2.3.3). The interplay of amplitude and phase can be seen by substituting Eq. (1) into Eq. (6) and by holding constant the amplitudes or the phases, respectively. Thus, non-zero coherence always indicates the presence of phase coupling, while it is hardly possible to infer directly from the coherence value to what extent amplitude coupling may also be involved.

2.3.2. Phase consistency

Since amplitude and phase contributions to coherence cannot be easily dissociated, it is sometimes enlightening to investigate these parameters separately. If one wants to focus, e.g., on the signals' phasing, amplitude contributions have to be eliminated in Eq. (5) or (6), respectively. For this purpose, only the spectra's phase factors (cf. Eq. (1)) are retained. Thus, coherence from Eq. (6) becomes *phase consistency*:

$$\begin{aligned}\kappa^2_{\varphi,XY}(f,t) &= \frac{\left|\sum_{n=1}^{N} \mathrm{e}^{\mathrm{i}\varphi_{X,n}(f,t)} \cdot \mathrm{e}^{-\mathrm{i}\varphi_{Y,n}(f,t)}\right|^2}{\sum_{n=1}^{N} 1^2 \cdot \sum_{n=1}^{N} 1^2} \\ &= \frac{1}{N^2}\left|\sum_{n=1}^{N} \mathrm{e}^{\mathrm{i}(\varphi_{X,n}(f,t)-\varphi_{Y,n}(f,t))}\right|^2,\end{aligned}$$

where $\varphi_{X,n}(f,t)$ and $\varphi_{Y,n}(f,t)$ denote the spectral phases of signal X and Y, respectively. Analogously to coherence, the *unsquared* version of phase consistency is usually more suitable for comparisons among different coupling measures:

$$\kappa_{\varphi,XY}(f,t) = \frac{1}{N}\left|\sum_{n=1}^{N} \mathrm{e}^{\mathrm{i}(\varphi_{X,n}(f,t)-\varphi_{Y,n}(f,t))}\right|. \tag{8}$$

Furthermore, as phase consistency is just a special case of coherence, the bias correction according to Eq. (7) remains valid; $\kappa^2_{\varphi,XY}(f,t)$ just has to be substituted for $\kappa^2_{XY}(f,t)$.

Phase consistency need not be regarded as a special case of coherence (like above), but can also be derived from a more general phase-locking condition (Rosenblum et al., 1996). Eq. (8) represents the most commonly used form of phase consistency. In literature, this measure has also been termed *phase locking* (*value*) or *phase synchrony*/*-ization* (e.g., Lachaux et al., 1999; Le Van Quyen et al., 2001; Mormann et al., 2000; Rodriguez et al., 1999; Tass et al., 1998).

2.3.3. Envelope correlation

Instead of focusing on the signals' phasing, it can as well be instructive to look at interactions among their amplitudes. With the previous section in mind, it would be most consistent to eliminate phase contributions in Eqs. (5) and (6) by retaining only the spectra's amplitude factors (cf. Eq. (1)). However, since this would result in an amplitude correlation coefficient *without* prior subtraction of the amplitudes' mean values, and since amplitudes are by definition always positive, such a measure would always be greater than zero, even for completely independent amplitude values. Therefore, the classical Pearson correlation coefficient between

amplitude values (including prior subtraction of the means) would be more appropriate.

However, this coupling measure would require amplitude ratios to be constant across single trials. When focusing on neurophysiological investigations, slow fluctuations of the system's general state (like, e.g., some-minute-scale changes in arousal) might induce local activation changes, which in turn could lead to a different development over time of signal amplitudes at different sites. As a consequence, the ratio between amplitudes at these sites would not be constant across single trials. In the previous sections, such a constancy was admittedly assumed for *phase differences* (as they are incorporated in coherence or phase consistency). In fact, this assumption seems plausible because phase differences are likely to reflect neuronal transmission delays, and conduction velocities along nerve fibers will usually not be strongly affected by the aforementioned slow fluctuations of state. With regard to signal *amplitude*, however, it is more plausible to assume that functional interactions are reflected in transiently covarying amplitudes on a smaller temporal scale, i.e., within a relatively short time interval. In many situations, therefore, it seems more preferable to quantify amplitude coupling by means of a different variant of correlation, which requires amplitude ratios to be constant during the (presumedly short) period of dynamic interaction, but not to be identical in each single trial. Such a (Pearson) cross-correlation of amplitude time courses, using a sliding time window, will be termed (*amplitude*) *envelope correlation* in the following.

Let

$$I_t = \{\tau | \tau \in [t - \tfrac{1}{2}T_\rho, t + \tfrac{1}{2}T_\rho)\} \tag{9}$$

be a correlation time window of length T_ρ, centered around time t, and let $\bar{A}^{(t)}_{X,n}(f)$ be the mean amplitude (at site X) within this time interval and within a frequency band centered around frequency f. Then the (time- and frequency-dependent) envelope-correlation coefficient for a given single trial n is

$$\rho_{A,XY,n}(f,t) = \frac{\sum_{\tau\in I_t}(A_{X,n}(f,\tau) - \bar{A}^{(t)}_{X,n}(f)) \cdot (A_{Y,n}(f,\tau) - \bar{A}^{(t)}_{Y,n}(f))}{\sqrt{\sum_{\tau\in I_t}(A_{X,n}(f,\tau) - \bar{A}^{(t)}_{X,n}(f))^2 \cdot \sum_{\tau\in I_t}(A_{Y,n}(f,\tau) - \bar{A}^{(t)}_{Y,n}(f))^2}}. \tag{10}$$

As in Section 2.1, the expectation value of this measure can be estimated by averaging across realizations. Since the Pearson correlation coefficient is a normalized quantity, averaging has to be performed on Fisher-Z-transformed values, and the result has to be transformed back:

$$\rho_{A,XY}(f,t) = \tanh\left(\frac{1}{N}\sum_{n=1}^{N}\tanh^{-1}(\rho_{A,XY,n}(f,t))\right). \tag{11}$$

This quantity has turned out to be a promising alternative to phase-sensitive coupling measures (Bruns et al., 2000). In contrast to coherence or phase consistency, it represents a non-linear form of signal coupling. Furthermore, the parameter space of its arguments can be expanded by two further dimensions (in addition to time and frequency). Firstly, the frequency f in Eq. (10) need not be identical for the two channels X and Y, so that, in general, it can be replaced by two different, independent center frequencies f_X and f_Y. This allows investigation of interactions between processes running at different frequencies. Secondly, the correlation *coefficient* can be generalized to a correlation *function*, which additionally regards non-zero time-lags between the amplitude envelopes.

3. Formal comparison of the approaches

3.1. Getting the spectro-temporal representation

There are several different possibilities for determining a signal's spectro-temporal representation. The most fundamental distinction is between those approaches which are model-based and those which are not. Model-based (e.g., autoregressive) techniques are not considered in the present report. Instead, the focus will be on the three most commonly used techniques which estimate amplitude and phase as direct signal parameters. These techniques are the *Fourier*, *Hilbert*, and *wavelet* approach, respectively, and will be reviewed in the following sections.

3.1.1. Fourier analysis

Fourier-based time-resolved spectral analysis (also called *short-time Fourier analysis*) requires a sliding time window and—in order to avoid spectral leakage and other undesirable effects—a window function $w^{(F)}(t)$ with smooth flanks (with (F) denoting *F*ourier-based analysis), which is multiplied with the signal segment defined by the time window. The choice of the window function has an effect on the outcome of the analysis, which is broadly discussed by Harris (1978). Good window functions fulfill at least three criteria: narrow bandwidth in the frequency domain, low sidelobe levels in the frequency domain, and no severe reduction of signal-to-noise ratio. In cases where absolute (as opposed to relative) signal power is of interest and should be preserved, the window function has to be divided by its own energy. In this report, however, such scaling is generally not considered because it is irrelevant with respect to a fundamental comparison of different analysis approaches.

For any given time window centered around time t, the signal $s(\tau)$ is multiplied by the window function $w^{(F)}(\tau - t)$, the product of which is then subjected to a discrete Fourier transform $\boldsymbol{F}$, with t serving as parameter. The transform yields the complex-valued, time- and

frequency-dependent spectrum

$$S^{(F)}(f,t) = \boldsymbol{F}_\tau\{s(\tau)\cdot w^{(F)}(\tau - t)\}. \quad (12)$$

The time–frequency representation becomes quasi-continuous in the time domain if the step width between successive time windows is chosen equal to the original sampling interval of the signal. In the frequency domain, any desired interpolation density can be achieved with the *padding* technique, in which the windowed signal segment is artificially extended by attaching additional zeroes to it before performing the Fourier transform (e.g., Harris, 1998). Note that neither the step width between time windows nor the frequency interpolation factor determined by the amount of padded values has any influence on the actual time–frequency resolution of $S^{(F)}(f,t)$. This depends solely on the length T_F of the sliding time window, and to a lesser degree on the shape of the chosen window function, but on nothing else.

3.1.2. Hilbert analysis

In the previous section, the signal $s(t)$ was decomposed into successive time epochs, and a Fourier spectrum was computed of each epoch. Alternatively, a spectro-temporal representation of the signal may be obtained by decomposing it into neighboring frequency components (i.e. bandpass signals) and by computing the so-called *analytic signal* of each component via the Hilbert transform. I will call this procedure the Hilbert approach.

The first step in computing the analytic signal for a given frequency band is to treat the original signal with a corresponding bandpass filter. This can be done by convolution with a filter kernel in the time domain or by multiplication with a transfer function in the frequency domain. In order to emphasize the concept of decomposing the signal into frequency components, I will use the latter alternative. The Fourier spectrum $S(\nu)$ of the original signal is multiplied by the transfer function $B_f(\nu)$, i.e. the bandpass filter in the frequency domain, which yields the bandpass spectrum

$$S_f(\nu) = S(\nu)\cdot B_f(\nu), \quad (13)$$

from which in turn the desired bandpass signal can be obtained by inverse Fourier transform:

$$s_f(t) = \boldsymbol{F}_\nu^{-1}\{S_f(\nu)\}. \quad (14)$$

The second step, which is the Hilbert transform, starts from the bandpass spectrum in Eq. (13). In the frequency domain, the Hilbert-transformed bandpass spectrum is given by

$$H_f(\nu) = -\mathrm{i}\,\mathrm{sgn}(\nu)\cdot S_f(\nu), \quad (15)$$

the inverse Fourier transform of which is the Hilbert-transformed bandpass signal

$$h_f(t) = \boldsymbol{F}_\nu^{-1}\{H_f(\nu)\}. \quad (16)$$

The bandpass signal $s_f(t)$ and its Hilbert transform $h_f(t)$ finally constitute the real and the imaginary part, respectively, of the *analytic signal*

$$S^{(H)}(f,t) = s_f(t) + \mathrm{i}h_f(t). \quad (17)$$

The superscript (H) indicates the Hilbert approach.

Due to the linearity of the Fourier transform, the spectrum of the analytic signal is

$$S_f(\nu) + \mathrm{i}H_f(\nu) = S_f(\nu)\cdot 2\varepsilon(\nu), \quad (18)$$

where $\varepsilon(\nu)$ denotes the Heavyside function (also called unit step function). This equality results from Eq. (15) in combination with the relation

$$1 + \mathrm{i}(-\mathrm{i}\,\mathrm{sgn}(\nu)) = (1 + \mathrm{sgn}(\nu)) = 2\varepsilon(\nu).$$

By substituting Eq. (13) into Eq. (18), the analytic signal (17) can also be written as

$$S^{(H)}(f,t) = \boldsymbol{F}_\nu^{-1}\{S(\nu)\cdot B_f(\nu)\cdot 2\varepsilon(\nu)\}. \quad (19)$$

This calculation rule allows obtaining the complete analytic signal from only one (inverse) Fourier transform, instead of computing its real and imaginary part separately via Eqs. (14)–(16). It is therefore advisable to use this calculation method whenever computational efficiency is a limiting factor.

The analytic signal (19) again constitutes a complex spectro-temporal representation of the original signal $s(t)$, specifying its amplitude and phase as a function of time and frequency. It is therefore equivalent to the expression in Eq. (12), which will be demonstrated in more detail in Section 3.2.

The analytic signal (19) is quasi-continuous in the time domain, since the employed operations do not change the sampling interval. In the frequency domain, any desired interpolation density can be achieved by choosing an appropriate step width for the center frequencies of the bandpass-filter transfer functions. As with the Fourier approach, however, the actual time–frequency resolution of the final result depends neither on the sampling frequency in the time domain nor on the step width in the frequency domain. In particular, it is a common misunderstanding that the temporal resolution of the analytic signal be equal to its sampling interval, which is definitely not the case. The resolution is solely determined by the bandwidth of the employed bandpass filter, and to a lesser degree by the exact shape of its transfer function.

3.1.3. Wavelet analysis

A third possibility to obtain a spectro-temporal representation of the signal $s(t)$ is to perform a wavelet analysis. In this approach, the signal is convolved with a number of filter kernels $w_f(t)$, called *wavelets*, that represent neighboring frequency bands. It is important to bear in mind that the present report only focuses on a certain class of wavelets, namely on the wavelet type usually preferred for spectral analyses. This type is a complex-valued oscillation $\mathrm{e}^{\mathrm{i}2\pi ft}$

multiplied by a bell-shaped (real-valued) envelope $a_f^{(W)}(t)$:

$$w_f(t) = a_f^{(W)}(t) \cdot e^{i2\pi ft}. \quad (20)$$

Thus, in much the same way that the Hilbert approach requires a bank of bandpass filters, the wavelet approach requires a family of wavelets, each representing a certain frequency band. Convolution (denoted by '*') of the original signal $s(t)$ with a wavelet $w_f(t)$ yields a complex signal

$$S^{(W)}(f,t) = s(t) * w_f(t), \quad (21)$$

which is the equivalent of the analytic signal in Eq. (19), as will be shown in the next section.

The bandwidth in wavelet analyses is typically chosen to increase proportionally with the oscillation frequency f of the wavelet. Thus, the constant parameter is not the *absolute*, but the *relative* time–frequency resolution (i.e., compared to the cycle period or the frequency, respectively). Equivalently, one may consider as the constant parameter the effective number of oscillation cycles that is used to estimate the amplitude and phase of the signal at any given point in time–frequency space. Again, although the original sampling interval in the time domain is preserved during the wavelet transform, the temporal resolution of the method is solely determined by the (frequency-dependent) wavelet length. The same holds for the frequency resolution, which does not (!) depend on the sampling density (i.e. step width) in the frequency domain.

3.2. Comparison of Fourier, Hilbert and wavelet analysis

The proportional relationship between bandwidth and frequency is often emphasized as being one of the most important advantages of the wavelet approach. However, such proportionality can as well be realized with the two other types of spectral analysis. In the Hilbert approach, the bandwidth Δf may be adapted to the center frequency f in any way wanted. The discrete Fourier transform, if implemented as the fast Fourier transform (FFT), cannot be evaluated separately for single frequencies, and the bandwidth has a constant value (independent of frequency) for a given window length T_F. Thus, for each frequency of interest, the analysis would have to be repeated with an appropriate window length, which is an admittedly inefficient, but feasible procedure. Alternatively, in order to compute spectral values in each of these sweeps only at the relevant frequency (and not across the whole range up to the Nyquist frequency, which would produce a lot of unnecessary values), it might be advisable to evaluate the discrete Fourier transform explicitly instead of using the FFT algorithm. But this is only a technical question.

A proportional relationship between bandwidth and center frequency might be particularly desirable in EEG or MEG analysis, because the classical brain-signal frequency bands (δ, ϑ, α, β, γ) roughly represent a logarithmic subdivision of the frequency axis. If, on the other hand, the neurophysiological processes to be investigated are assumed to occur on a certain temporal scale, it seems more appropriate for analysis to use a fixed, i.e., frequency-independent temporal resolution in the expected time range. Thus, there is no general rule as to whether the analysis bandwidth should or should not scale with center frequency, and correspondingly, none of the above-mentioned approaches can a priori be regarded as "more suitable" in this respect than the others.

Therefore, it is more interesting to ask what are, from the theoretical point of view, the most important *inherent* differences among the Fourier, Hilbert and wavelet technique, i.e., those differences that remain when the three methods are matched with each other with respect to their analysis bandwidth or, equivalently, to their temporal resolution. The answer may be surprising: Although the three different algorithms presented in the preceding sections suggest that the three analysis techniques are thoroughly different, they are in fact essentially equivalent. Both Fourier and Hilbert transform can be expressed as convolution of the original signal with a complex oscillatory kernel, just like the wavelet transform according to Eq. (21).

The formal equivalence of Fourier and wavelet analysis can be seen as follows. For a given time window centered around t and for a given discrete frequency value f, the explicit evaluation of Eq. (12), using the definition of the discrete Fourier transform, yields

$$S^{(F)}(f,t) = \sum_{t-\frac{1}{2}T_F \le \tau < t+\frac{1}{2}T_F} (s(\tau) \cdot w^{(F)}(\tau - t)) \cdot e^{-i2\pi f\left(\tau - t + \frac{T_F}{2}\right)}. \quad (22)$$

If the window function is symmetric (which is usually the case), the sign of its argument can be inverted: $w^{(F)}(\tau - t) = w^{(F)}(t - \tau)$. Additionally, due to the associativity of multiplication, the large parentheses on the right-hand side of Eq. (22) can be rearranged, so that each summand is not interpreted as the windowed signal multiplied by a complex oscillation, but instead as the original signal multiplied by an oscillatory kernel:

$$S^{(F)}(f,t) = \sum_{t-\frac{1}{2}T_F \le \tau < t+\frac{1}{2}T_F} s(\tau)\left(w^{(F)}(t - \tau) \cdot e^{i2\pi f\left(\tau - t + \frac{T_F}{2}\right)}\right). \quad (23)$$

The entire sum thus turns out to be the convolution product (*) of the original signal and an oscillatory kernel whose envelope is given by the window function:

$$S^{(F)}(f,t) = s(t) * \left(w^{(F)}(t - \tau) \cdot e^{i2\pi f\left(\tau - t + \frac{T_F}{2}\right)}\right). \quad (24)$$

In this form, the equivalence of Fourier and wavelet approach is easily seen, with the term in large parentheses in Eq. (24) corresponding to the wavelet $w_f(t)$ in Eq. (21). Of course, this equivalence also holds for frequencies f that lie *between* the regular sampling points of the discrete Fourier transform,

or in other words, that are only accessible through interpolation of the Fourier spectra by means of (zero-) padding (cf. Section 3.1.1).

For demonstrating the equivalence of Hilbert and wavelet analysis, it is helpful to introduce the concept of the *equivalent lowpass*. For any symmetric bandpass with a transfer function $B_f(\nu)$ centered around frequency f, the equivalent lowpass $B_T(\nu)$ is obtained by re-centering the positive (or the negative) branch of the transfer function around frequency zero and multiplying it by 2:

$$\begin{aligned} B_T(\nu) &= B_f(\nu + f) \cdot 2\varepsilon(\nu + f) \\ &= B_f(\nu - f) \cdot 2(1 - \varepsilon(\nu - f)). \end{aligned} \tag{25}$$

Inversely, the actual bandpass transfer function can then be expressed as

$$B_f(\nu) = \tfrac{1}{2} B_T(\nu - f) + \tfrac{1}{2} B_T(\nu + f). \tag{26}$$

Thus, the term $B_f(\nu)2\varepsilon(\nu)$ in Eq. (19) can be written as convolution of the transfer function of the equivalent lowpass $B_T(\nu)$ with a delta function centered at frequency f:

$$\begin{aligned} B_f(\nu) \cdot 2\varepsilon(\nu) &= \underbrace{B_T(\nu - f) \cdot \varepsilon(\nu)}_{=B_T(\nu - f)} + \underbrace{B_T(\nu + f) \cdot \varepsilon(\nu)}_{=0} \\ &= B_T(\nu) * \delta(\nu - f). \end{aligned} \tag{27}$$

Furthermore, using the convolution theorem, the first of the two frequency-domain products in braces on the right-hand side of Eq. (19) can be transformed into a time-domain convolution, such that Eq. (19) as a whole takes a form equivalent to Eq. (21):

$$\begin{aligned} S^{(H)}(f, t) &= s(t) * \boldsymbol{F}_{\nu}^{-1}\{B_T(\nu) * \delta(\nu - f)\} \\ &= s(t) * (b_T(t) \cdot \mathrm{e}^{\mathrm{i}2\pi f t}). \end{aligned} \tag{28}$$

where $b_T(t)$ is the equivalent-lowpass impulse response of the employed filter. Again, as in Eq. (24), the term in large parentheses on the right-hand side of Eq. (28) corresponds to the wavelet $w_f(t)$ in Eq. (21).

Another alternative of demonstrating the equivalence of Hilbert and wavelet approach has been given by Quiroga et al. (2002), who argued that the real and the imaginary part of a signal's wavelet transform correspond to the bandpass-filtered signal and its Hilbert transform, respectively. While this argumentation holds both for phase and amplitude estimation, the authors did not include the latter in their considerations, as their interest was directed towards synchronization measures.

In summary, Fourier, Hilbert and wavelet approach yield formally equivalent spectro-temporal representations of a given signal, as can be seen from a direct comparison of Eqs. (24), (28) and (21)/(20):

$$\begin{aligned} S^{(F)}(f, t) &= s(t) * \left(w^{(F)}(t) \cdot \mathrm{e}^{\mathrm{i}2\pi f \left(t - \frac{T_F}{2}\right)} \right) \\ S^{(H)}(f, t) &= s(t) * (b_T(t) \cdot \mathrm{e}^{\mathrm{i}2\pi f t}) \\ S^{(W)}(f, t) &= s(t) * (a_f^{(W)}(t) \cdot \mathrm{e}^{\mathrm{i}2\pi f t}) \end{aligned} \quad . \tag{29}$$

In each case, the time-resolved spectral analysis is mathematically equivalent to convolution of the original signal $s(t)$ with an amplitude-modulated complex oscillatory kernel $\mathrm{e}^{\mathrm{i}2\pi f t}$ (which is phase-shifted by a constant factor $\mathrm{e}^{-\mathrm{i}\pi f T_F}$ in Fourier analysis). The difference between the analysis approaches solely concerns the shape of the kernel envelopes, which is up to the user. In wavelet analysis, the envelope is often chosen to be a Gaussian ($\mathrm{e}^{-t^2/2\sigma_t^2}$; cf. Section 4.1), in Fourier analysis, it is the window function $w^{(F)}(t)$, and in Hilbert analysis, it is the equivalent-lowpass impulse response $b_T(t)$ of the employed filter. Therefore, choosing among the different analysis approaches amounts to the same question as, for example, choosing among different window functions in short-time Fourier analysis.

In many articles, there are statements to the effect that the wavelet approach, unlike the Fourier approach, does not require stationary signals (e.g., Lachaux et al., 1999, 2002; Nikolaev et al., 2001), or that the Hilbert approach characterizes time-dependent signal amplitude more precisely than the Fourier approach (e.g., Clochon et al., 1996, Freeman and Rogers, 2002). Depending on their context, such statements are at least misleading and sometimes even incorrect. The same holds all the more for sweeping statements such as one of the approaches being generally preferable to the others.

4. Empirical comparison of the approaches

Section 2 has been devoted to the most common measures which can be derived from a signal's complex-valued spectro-temporal representation, regardless of the applied analysis approach. In Section 3, the formal equivalence of Fourier, Hilbert and wavelet spectral analyses has been demonstrated. This section now is meant to show, by means of a quantitative comparison, that the three approaches also yield largely comparable results for typical parameter settings used *in practice*. For this purpose, the convolution kernels according to Eq. (29) have to be specified in detail first.

4.1. Specification of filter parameters

4.1.1. Fourier approach

A well-established window function for short-time Fourier analysis is the so-called *Hamming* window, which, according to Harris (1978), is defined as

$$\begin{aligned} w^{(F)}(t) = w_{\mathrm{Hamming}}(t) &= \alpha + (1 - \alpha) \cos\left(\frac{2\pi}{T_F} t\right), \\ -\frac{T_F}{2} \le t < \frac{T_F}{2},\ \alpha &= \frac{25}{46}, \end{aligned} \tag{30}$$

where T_F is the window's length in the time domain. (Of course, several other window functions would as well be

suitable.) In this example, the kernel in large parentheses in Eq. (29) becomes

$$w^{(F)}(t, f) = w_{\text{Hamming}}(t) \cdot \mathrm{e}^{\mathrm{i}2\pi f\left(t-\frac{T_F}{2}\right)}. \tag{31}$$

4.1.2. Hilbert approach

For the Hilbert approach, a bandpass transfer function $B_f(\nu)$ has to be specified. For didactic reasons, it is most suggestive to start from an ideal bandpass (i.e., a rectangle function of frequency), and to modify its (initially vertical) flanks in such a way that the corresponding time-domain kernel shows less overshoot and decays more rapidly with time. In the present report, flanks are chosen to be $\cos^2$-shaped, and their positions are determined by the fact that the cut-off frequencies $f - \Delta f$ and $f + \Delta f$ are supposed to mark the 3 dB points. Furthermore, to simplify matters, the total width of each flank is given the same value Δf as the half-bandwidth of the filter, which ensures a reasonable compromise between a small time-domain overshoot on the one hand and a sharp pass-band boundary on the other hand. Formally, this transfer function is most easily described through its equivalent lowpass (cf. Section 3.2, Eqs. (25) and (26)):

$$B_T(\nu) = 2\begin{cases} \cos^2\left(\frac{\pi}{2}\frac{\nu+\Delta f_\mathrm{p}}{\Delta f}\right), & -\Delta f_\mathrm{p} - \Delta f < \nu < -\Delta f_\mathrm{p} \\ 1, & -\Delta f_\mathrm{p} \le \nu \le \Delta f_\mathrm{p} \\ \cos^2\left(\frac{\pi}{2}\frac{\nu-\Delta f_\mathrm{p}}{\Delta f}\right), & \Delta f_\mathrm{p} < \nu < \Delta f_\mathrm{p} + \Delta f \end{cases}, \tag{32}$$

where (without proof)

$$\Delta f_\mathrm{p} = \frac{2}{\pi}\arcsin(10^{-0.15}) \cdot \Delta f \approx 0.5 \cdot \Delta f$$

is the half-width of the ideal proportion of the pass-band (i.e., without flanks). Finally, the shape of the convolution kernel is given by the equivalent-lowpass impulse response $b_T(t)$:

$$w^{(H)}(t, f) = b_T(t) \cdot \mathrm{e}^{\mathrm{i}2\pi ft}. \tag{33}$$

For this special filter, the shape of the impulse response $b_T(t)$ can be given in analytical form, but the expression is not very intuitive, so that its graphical depiction (Fig. 1) appears much more meaningful.

4.1.3. Wavelet approach

The most commonly used wavelet type for spectral analyses is the *Gabor* or *Morlet* wavelet, in which the envelope $a_f^{(W)}(t)$ in Eq. (20) is a Gaussian ($\mathrm{e}^{-t^2/2\sigma_t^2}$). The time-domain standard deviation σ_t of this wavelet is inversely proportional to the standard deviation $\sigma_f = 2\pi/\sigma_t$ of its frequency-domain representation (which is also Gaussian), and the latter scales proportionally with frequency f. The (constant) ratio f/σ_f determines the effective number of oscillation cycles comprised in the wavelet.

Analogously to Eqs. (31) and (33), the convolution kernel for wavelet analysis is given by

$$w^{(W)}(t, f) = \mathrm{e}^{-t^2/2\sigma_t^2} \cdot \mathrm{e}^{\mathrm{i}2\pi ft} \tag{34}$$

The three filter-kernel envelopes from Eqs. (31), (33) and (34) can be directly compared when they are scaled to equal sizes in the time or frequency domain, e.g., to equal 3-dB half-bandwidths Δf. In Hilbert analysis, Δf is explicitly included in the filter construction formula according to Eq. (32). In the two other approaches, the bandwidths of the transfer functions can be (analytically) expressed through the parameters T_F (window length) and σ_f (frequency-domain standard deviation), respectively. The approximate values are:

$$\begin{aligned} \Delta f^{(F)} &\approx \frac{0.899}{T_F} \\ \Delta f^{(H)} &= \Delta f \\ \Delta f^{(W)} &\approx 1.175\sigma_f \end{aligned} \quad . \tag{35}$$

Fig. 1 shows a graphical comparison of the Fourier, Hilbert and wavelet convolution kernels, with center frequencies and bandwidths being matched with each other. Note that the

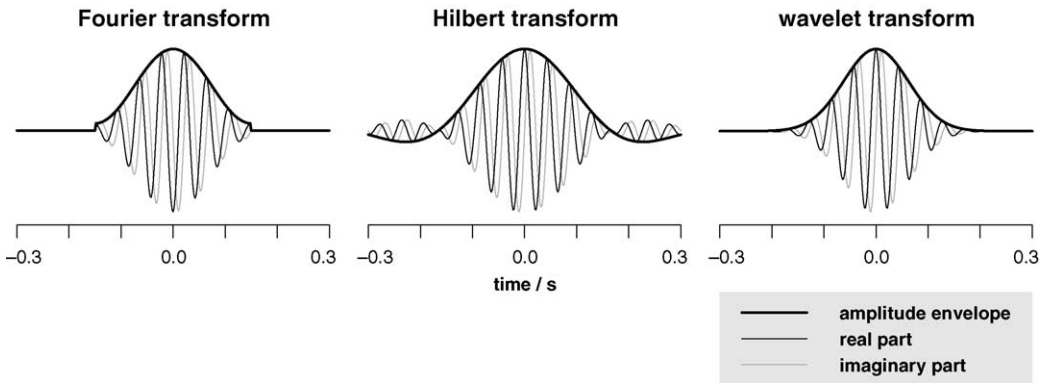

Fig. 1. Both Fourier and Hilbert transform are mathematically equivalent to convolution of the original signal with complex oscillatory kernels, just as is wavelet transform by definition. Filter kernels of the three approaches are very similar when analysis parameters are chosen appropriately. Illustrations show kernels for the examples specified in the text (Hamming window for Fourier analysis, ideal bandpass with smooth flanks for Hilbert analysis, Gaussian envelope for wavelet analysis). Curves show real and imaginary parts as well as envelopes of the complex kernels for center frequency 23.3 Hz and 3 dB half-bandwidth 3.0 Hz.

differences among the three analysis approaches can really be put down to the differences seen in this illustration. The larger overshoot of the Hilbert kernel compared to the other kernels is due to the finite width of its ideal pass-band in the frequency-domain. By choosing a Gaussian window function for Fourier analysis and a Gaussian frequency-domain transfer function for Hilbert analysis, the three approaches could have been made even perfectly identical. In this example, however, different filter forms have been chosen deliberately, in order to demonstrate that despite these differences, results are still very similar.

4.2. Comparison of spectral amplitude

Since spectral amplitude is one of the most commonly used signal parameters, its sensitivity to the different analysis approaches is probably of particular interest. As an example, I will consider electrical brain signals that were recorded with subdurally implanted electrodes directly from the cortical surface of epileptic patients undergoing presurgical evaluation of their epileptogenic foci (lowpass 70 Hz, sampling rate 200 Hz; for details, see Bruns et al., 2000; Bruns and Eckhorn, 2004). Fig. 2 shows a 3 s signal segment and its amplitude time courses at three different center frequencies f and bandwidths Δf, respectively. Note that in this example, bandwidths are chosen to scale proportionally with center frequency, which leads to the higher temporal resolution at higher center frequencies.

As one can see, the amplitude time courses are virtually identical, while the slight differences are due to the slightly different shapes of the explicitly or implicitly used filter kernels (Fig. 1). In order to empirically confirm the high similarity of the three approaches on the basis of a bigger data set, a 50 s signal segment was randomly chosen from each electrode in 6 human subjects, yielding about 330 such segments altogether (and, thus, a data set 5500 times larger than the one in Fig. 2). For each segment, Fourier-, Hilbert- and wavelet-based amplitude time-courses were computed for three center frequencies (15, 30, and 60 Hz) and for 50 different *relative* bandwidths $\delta f = \Delta f/f$, respectively, covering the range $\delta f = 0.05, \ldots, 0.30$. Thus, for each analysis approach and for each relative bandwidth δf, approximately 1000 signal segments (of 50 s duration each) have been included in the following comparative analysis.

The classical Pearson correlation coefficient served as a measure of similarity among the amplitude time courses. It was estimated from the about 1000 realizations for every possible combination of relative bandwidths δf between the three analysis approaches. The result is shown in Fig. 3, in which each of the three matrices represents the comparison between two approaches, respectively. Bandwidths δf are varied along the matrices' axes, and the color-coded matrix elements show mean correlation coefficients between single-trial amplitude time courses, each obtained by averaging across the ∼1000 correlation coefficients from single realizations. If the three approaches were perfectly equiva-

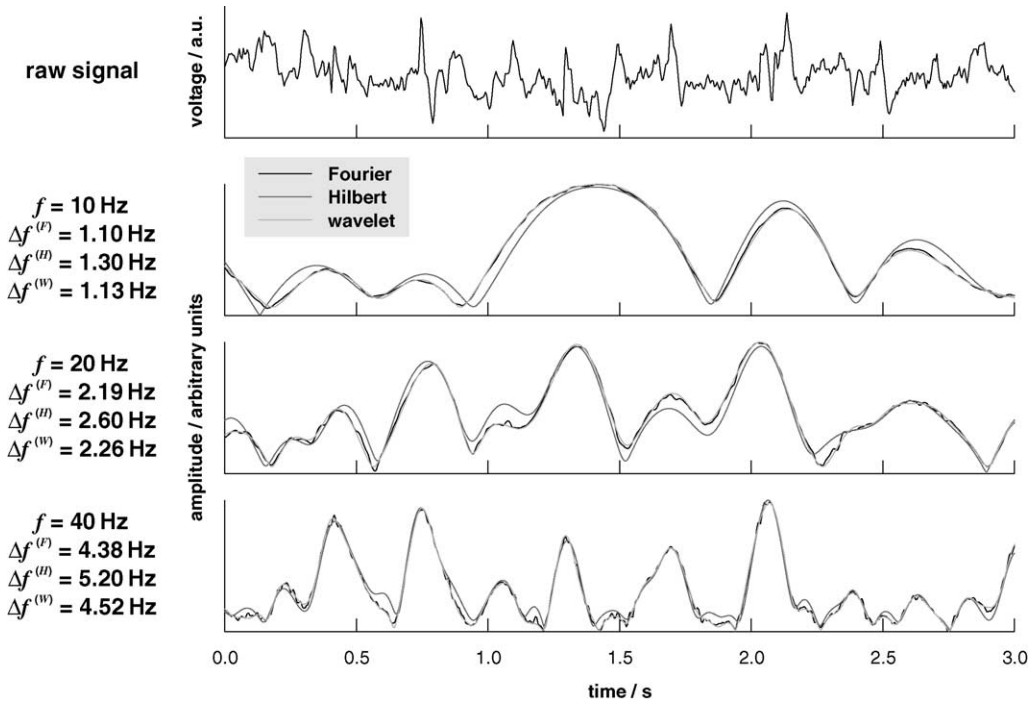

Fig. 2. Fourier-, Hilbert- and wavelet-based amplitude time courses are virtually congruent when center frequencies are identical and bandwidths are equivalent according to Eqs. (35) and (36). Top row: arbitrarily chosen raw signal segment of ongoing activity subdurally recorded over the occipital lobe in a human subject (sampling rate 200 Hz). Second to fourth row: amplitude time courses (normalized, i.e. not to scale) obtained from the above signal segment for different center frequencies and 3 dB half-bandwidths. For each of the three analysis approaches (curves within each diagram), slightly different bandwidth values were chosen according to Eq. (36) so as to achieve the best possible match among the approaches.

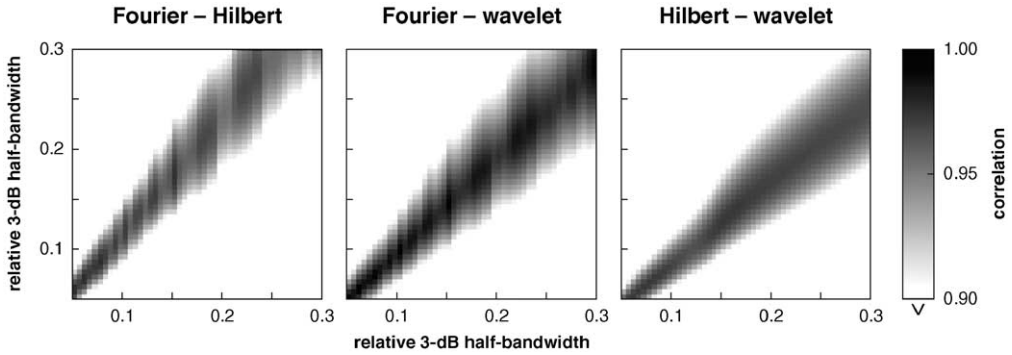

Fig. 3. Fourier-, Hilbert- and wavelet-based spectral analyses yield almost identical amplitude values as long as analysis parameters are matched with each other. Matrices show mean pairwise Pearson correlation coefficients between amplitude time courses from different analysis approaches, respectively, as a function of relative 3 dB half-bandwidths. Underlying data are subdural recordings (sampling rate 200 Hz, correlation time interval 50 s; averages across three center frequencies—15, 30, 60 Hz—and across 40–60 recording positions, respectively, in six human subjects). Note that the color scale starts at 0.9.

lent, correlation values along the matrix diagonals would be unity.

Maximal correlation values within the matrices are indeed very high and show only small variability among the six subjects and the three center frequencies. Maximal mean values ($\pm$ standard deviations across subjects and center frequencies, $N = 18$) are 0.971 ± 0.010, 0.993 ± 0.006 and 0.973 ± 0.003 for Fourier/Hilbert, Fourier/wavelet and Hilbert/wavelet comparison, respectively. Correlation values involving the Hilbert approach (Fig. 3, left and right matrix) are generally somewhat smaller, which is obviously due to the more deviant shape of the Hilbert convolution kernel (Fig. 1, middle). As mentioned above, higher correlation values could have been achieved by using a slightly different bandpass transfer function with a time-domain kernel more similar to that of the other approaches.

The apparent discontinuities in the matrices involving the Fourier approach (Fig. 3, left and middle matrix) result from the fact that the Fourier window length T_F, unlike the "Hilbert bandwidth" Δf or the wavelet standard deviation σ_f, can only take discrete values (determined by the sampling interval of 5 ms in the raw data). According to Eq. (35), then, the same holds for the (relative) bandwidth, such that the Fourier bandwidth $\delta f^{(F)}$ does not actually change with each single step of 0.005 along the abscissae.

Most strikingly, the highest correlation values in Fig. 3 are not precisely found along the matrix diagonals, but on straight lines with slopes slightly different from unity. The exact values of these slopes indicate those bandwidth ratios at which the best match between two analysis approaches is achieved, respectively. In detail, the mean ratios ($\pm$ standard deviations across subjects and center frequencies, $N = 18$) are

$$\begin{aligned} \frac{\delta f^{(W)}}{\delta f^{(H)}} &= 0.843 \pm 0.013, \\ \frac{\delta f^{(H)}}{\delta f^{(F)}} &= 1.150 \pm 0.014, \\ \frac{\delta f^{(F)}}{\delta f^{(W)}} &= 1.044 \pm 0.004. \end{aligned} \tag{36}$$

Again, there are larger deviations from unity when the Hilbert approach is involved. All deviations from unity (both of the slopes and of the maximal correlation coefficients) can be explained by the differences among the three convolution kernels (Fig. 1) and could be eliminated by choosing slightly different window functions, bandpass filters or wavelet envelopes, respectively.

4.3. Comparison of phase coupling

Apart from amplitude, phase as the other important spectral signal parameter is particularly interesting when phase-sensitive coupling measures are concerned (cf. Section 2.3). However, a detailed real-data-based comparison among the three analysis approaches with regard to the signals' phasing is dispensable in the present report, because such an investigation has partly been carried out previously by Le Van Quyen et al. (2001). They demonstrated the virtual equivalence of Hilbert- and wavelet-based phase consistency (cf. Section 2.3.2) for extracranially as well as intracranially recorded EEG signals. As part of a more comprehensive comparison among several different synchronization measures, also Quiroga et al. (2002) reported that Hilbert and wavelet transform yielded similar phase consistency values, in addition to pointing out their formal equivalence (cf. Section 3.2). Having in mind the formal equivalence of the three approaches according to Eq. (29) as well as the similarity of their convolution kernels (Fig. 1), these results of course are just as little surprising as the amplitude equivalence demonstrated in the previous section. For the same reason, additional consideration of short-time Fourier analysis in the studies of Le Van Quyen et al. or of Quiroga et al. would have yielded corresponding results and will not be detailed in the present report. The main goal of this article is to embed the existing comparisons concerning phase synchrony measures into a more general framework by extending the above studies to spectral amplitude, by explicitly incorporating the Fourier approach and by giving a general formal comparison among the three approaches.

5. Discussion

The concern of this article was to demonstrate that short-time Fourier transform, Hilbert transform and wavelet transform constitute formally and effectively equivalent spectral analysis approaches. This equivalence refers to phase as well as amplitude and thus also to all quantities derived from these two parameters of the complex spectro-temporal representation. The reason why the techniques are often regarded as being completely different lies in the way they are typically used.

Firstly, in many comparative studies, the approaches are not matched with each other with respect to their time–frequency resolution, i.e., window length or bandwidth, respectively (e.g., Clochon et al. (1996): Fourier- and Hilbert-based amplitude applied to brain signals; DeShazer et al. (2001): Hilbert- and wavelet-based phase synchrony applied to coupled laser array). The Fourier approach, for example, is mostly used for analysis of longer signal segments, the results of which of course are not comparable to those obtained with, e.g., much shorter wavelets. Therefore, it is absolutely necessary in such comparative studies to choose equivalent analysis parameters, i.e. identical *effective* bandwidths. In the example in this report (Section 4.1), the relevant parameters F_T and σ_f would have to be determined from the desired bandwidth Δf, using Eqs. (35) and (36).

Secondly, an important difference among the approaches refers to the way in which they are usually carried out in practice. Wavelet transforms are typically performed with a constant *relative* bandwidth $\delta f = \Delta f/f$, whereas in Fourier transforms the *absolute* bandwidth Δf is held constant, and the way of performing Hilbert-based analyses varies. The difference between δf and Δf being held constant is easily illustrated in a two-dimensional parameter space with frequency f as one dimension and bandwidth Δf as the other. In this space, a Fourier analysis would cover a line parallel to the frequency axis, whereas a wavelet analysis would cover an oblique line passing through the origin. Thus, neither of these alternatives can be said to cover a larger proportion of parameter space. In order to systematically scan a full $f \times \Delta f$ rectangle, both analyses would have to be repeated for several parameter values within a certain range.

It is a common misunderstanding that, e.g., wavelet analysis in principle offers a "better" trade-off between time and frequency resolution than Fourier analysis. Time–frequency uncertainty (i.e. the finite product of kernel length in time and filter bandwidth) cannot be circumvented by any spectral analysis method. It can only be *reduced* by choosing an appropriate filter-kernel shape, which, however, refers to all three approaches. The optimal (i.e. smallest) total uncertainty can be achieved with Gaussian filters (as used for wavelet analysis in Section 3.1), but such filters show other disadvantages instead, e.g., lower signal-to-noise ratios (Harris, 1978). Therefore, the only fundamental question is whether temporal and spectral resolution should or should not depend on frequency f. If neuronal processes reflected in higher signal frequency bands are also expected to show dynamics on a shorter temporal scale, then the first alternative is more appropriate. If, on the other hand, processes are expected to run on a certain (fixed) temporal scale, while the frequency band they are reflected in is not intricately linked to this scale, then the temporal resolution (and, thus, the bandwidth) should be chosen independent of frequency. Without an a-priori conceptual model in mind about the time scale on which the neuronal processes take place, it is not possible to say which method is more appropriate. In such cases, it is most advisable to fully scan a reasonably large proportion of frequency–bandwidth parameter space by repeatedly performing the preferred spectral analysis with different absolute or relative bandwidths, respectively.

Note that this argumentation deliberately disregards formal mathematical criteria like orthogonality or completeness of the basis functions, but instead is geared to the needs and questions typically occurring in neurophysiological signal analysis. It is not always sufficient to know, for example, that a certain spectral decomposition would allow full reconstruction of the original signal or interpolation of any desired value. In many situations, displaying or interpreting the results requires that the interpolation be really *carried out*, i.e., that spectro-temporal representations be highly oversampled in one or in both dimensions, irrespective of any possible redundancies. Note also that the term "wavelet analysis" in the present report is confined to the way it is typically used for spectral analyses, i.e., to the wavelet definition given in Eq. (20). Of course, wavelet analyses offer the possibility to define very specific, not necessarily oscillatory, convolution kernels which may serve, e.g., as templates in order to detect certain signal elements. Such cases are part of an entirely different story and are exempt from the above considerations.

Anyhow, once a decision has been made on the shape of the filter kernels or transfer functions, and on whether absolute or relative bandwidths are to be held constant, the final criterion for using one or the other of the three approaches is merely computational efficiency. In general, short-time Fourier transform is particularly fast when the number of samples within one time window is a power of 2. Apart from this, however, overall computational efficiency heavily depends on the window step width in Fourier analysis, on the length (and, therefore, tolerable error size) of the convolution kernel in wavelet analysis, and, most importantly, on the degree of time and frequency interpolation in all three approaches. Thus, prior to an extensive analysis, the computational costs of the different techniques should be compared under the given conditions.

In conclusion, most traditional single-channel as well as coupling analyses are based on a complex-valued spectro-temporal representation of the neurophysiological signals in question. Whether this representation is obtained via Fourier, Hilbert or wavelet transform, is actually of minor importance. It is much more decisive to search for or to choose a time–frequency resolution that most reliably allows detec-

tion of the desired neurophysiological processes. Manipulating the exact shape of the filter kernel (time domain) or transfer function (frequency domain) can then serve to optimize the quality of the outcome. Each of the three approaches is equally suited to perform such parameter adjustments.

Acknowledgements

I thank Professor Reinhard Eckhorn (Philipps University, Marburg, Germany) and Dr. Alexander Gail (Caltech, Pasadena, CA, USA) for their help in improving the manuscript. This work was supported by the Deutsche Forschungsgemeinschaft (German Research Foundation; grant no. EC 53/9-3 given to Reinhard Eckhorn).

References

Adrian ED, Matthews BHC. The Berger rhythm: potential changes from the occipital lobes in man. Brain 1934;57:355–85.

Bendat JS, Piersol AG. Random data: analysis and measurement procedures. New York: Wiley; 1971.

Benignus VA. Estimation of the coherence spectrum and its confidence interval using the fast Fourier transform. IEEE Trans Aud Electroacoust 1969;AU-17:145–50.

Berger H. Über das Elektroenkephalogramm des Menschen: 1. Mitteilung Archiv für Psychiatrie und Nervenkrankheiten 1929;87:527–70.

Bruns A, Eckhorn R. Task-related coupling from high- to low-frequency signals among visual cortical areas in human subdural recordings. Int J Psychophysiol 2004;51:97–116.

Bruns A, Eckhorn R, Jokeit H, Ebner A. Amplitude envelope correlation detects coupling among incoherent brain signals. NeuroReport 2000;11:1509–14.

Clochon P, Fontbonne JM, Lebrun N, Etévenon P. A new method for quantifying EEG event-related desynchronization: amplitude envelope analysis. Electroencephalogr Clin Neurophysiol 1996;98: 126–9.

DeShazer DJ, Breban R, Ott E, Roy R. Detecting phase synchronization in a chaotic laser array. Phys Rev Lett 2001;87:044101.

Freeman WJ, Rogers LJ. Fine temporal resolution of analytic phase reveals episodic synchronization by state transitions in gamma EEGs. J Neurophysiol 2002;87:937–45.

Harris FJ. On the use of windows for harmonic analysis with the discrete Fourier transform. Proc IEEE 1978;66:51–83.

Harris CM. The Fourier analysis of biological transients. J Neurosci Methods 1998;83:15–34.

Lachaux JP, Rodriguez E, Martinerie J, Varela FJ. Measuring phase synchrony in brain signals. Hum Brain Mapp 1999;8:194–208.

Lachaux JP, Lutz A, Rudrauf D, Cosmelli D, Le van Quyen M, Martinerie J, Varela F. Estimating the time-course of coherence between single-trial brain signals: an introduction to wavelet coherence. Neurophysiologie Clinique 2002;32:157–74.

Le Van Quyen M, Foucher J, Lachaux JP, Rodriguez E, Lutz A, Martinerie J, Varela FJ. Comparison of Hilbert transform and wavelet methods for the analysis of neuronal synchrony. J Neurosci Methods 2001;111:83–98.

Mormann F, Lehnertz K, David P, Elger CE. Mean phase coherence as a measure for phase synchronization and its application to the EEG of epilepsy patients. Physica D 2000;144:358–69.

Nikolaev AR, Ivanitsky GA, Ivanitsky AM, Posner MI, Abdullaev YG. Correlation of brain rhythms between frontal and left temporal (Wernicke's) cortical areas during verbal thinking. Neurosci Lett 2001;298:107–10.

Quiroga RQ, Kraskov A, Kreuz T, Grassberger P. Performance of different synchronization measures in real data: a case study on electroencephalographic signals. Phys Rev E 2002;65:041903.

Rodriguez E, George N, Lachaux JP, Martinerie J, Renault B, Varela FJ. Perception's shadow: long-distance synchronization of human brain activity. Nature 1999;397:430–3.

Rosenblum MG, Pikovsky AS, Kurths J. Phase synchronization of chaotic oscillators. Phys Rev Lett 1996;76:1804–7.

Tass P, Rosenblum MG, Weule J, Kurths J, Pikovsky A, Volkmann J, Schnitzler A, Freund HJ. Detection of n:m phase locking from noisy data: application to magnetoencephalography. Phys Rev Lett 1998;81:3291–4.